Major article

E-cadherin redistribution mediated by *Clostridioides difficile* toxins increases spore-association to adherens junctions.

Pablo Castro-Córdova[1,2,#], Macarena Otto-Medina[1,#], D Borden Lacy[3], Daniel Paredes-Sabja [2,4*]

[#] Both authors contributed equally to this work.

[1] Departamento de Ciencias Biológicas, Facultad de Ciencias de la Vida, Universidad Andrés Bello, Santiago, Chile.

[2] ANID – Millennium Science Initiative Program – Millennium Nucleus in the Biology of the Intestinal Microbiota, Santiago, Chile.

[3] Department of Pathology, Microbiology, and Immunology, Vanderbilt University School of Medicine, Nashville, Tennessee, USA.

[4] Department of Biology, Texas A&M University, College Station, Texas, USA.

Short Title: Association of *C. difficile* spores to adherens junctions.

Word Count

Abstract: 148 words

Text (introduction, methods, results, and discussion): 3493 words

References: 50

ABSTRACT

Nearly ~20% of patients with *C. difficile* infection (CDI) manifest recurrence of CDI (R-CDI). During CDI, *C. difficile* forms spores essential for R-CDI. Interactions of *C. difficile* spores with intestinal epithelial cells (IECs) contribute to R-CDI. However, this interaction remains poorly understood. Here, we provide evidence that *C. difficile* spores interact with E-cadherin, contributing to spore-adherence and internalization into IECs. *C. difficile* toxins TcdA/TcdB lead to adherens junctions opening and increase spore-adherence to IECs. Confocal micrographs demonstrate that *C. difficile* spores associate with accessible E-cadherin; spore-E-cadherin association increases upon TcdA/TcdB intoxication. The presence of anti-E-cadherin antibodies decreased spore adherence and entry into IECs. By ELISA, immunofluorescence, and immunogold labelling, we observed that E-cadherin binds to *C. difficile* spores, specifically to the hair-like projections of the spore. Overall, these results expand our knowledge of how *C. difficile* spores bind to IECs and how toxin-mediated damage affects spore interactions with IECs.

Key Words:

C. difficile spores, E-cadherin, spore-host interaction, *C. difficile* toxins TcdA/TcdB.

INTRODUCTION

C. difficile is a Gram-positive, anaerobic, spore-forming bacterium and the main causative agent of antibiotic-associated diarrhea, causing death in ~5% of cases (1, 2). R-CDI is a major clinical challenge affecting ~30% of CDI patients (2, 3). CDI is primarily driven by the *C. difficile* toxins TcdA and TcdB, with contributions from the binary transferase toxin in some cases (4-6). Both TcdA and TcdB target their intracellular glucosyltransferase activity towards RhoA, Rac1, and Cdc42 (7, 8). This inhibitory modification of the Rho GTPase family leads to actin depolymerization and disruption of tight and adherens junctions (9-13), causing disruption of epithelial paracellular barrier function (14). Clinical studies shown that administration of anti-TcdB antibody (bezlotoxumab) in combination with antibiotics reduces R-CDI rates (15). The antibody may prevent toxin-mediated stem cell dysfunction and therefore prevent the delay in recovery and repair of the intestinal epithelium (10).

During infection, *C. difficile* produces spores (16); strains unable to form spores do not cause R-CDI in animal models (17), being the spores critical for R-CDI. EDTA-disruption of cell-cell junctions of Caco-2 cells leads to increased adherence of *C. difficile* spores to the cell-cell junction, suggesting a tropism for cell-cell junctions (18). *C. difficile* spores bind to fibronectin and vitronectin, located in the basolateral membrane (19). These molecules contribute to *C. difficile* spore internalization into IECs in an integrin-dependent manner, and spore-entry *in vivo* contributes to the R-CDI (20).

The intestinal barrier is an impermeable layer that separates the apical and basolateral cell sides (21), formed by junctions between adjacent IECs. The cell-cell junctions between IECs are

constituted of E-cadherin containing adherens junctions and tight junctions formed by claudins, occludins, and zonula occludens. These junctions provide the gut barrier with impermeability properties and restrict the translocation of pathogens and commensal bacteria. However, some pathogens can alter or disrupt the cell junctions, to translocate through the host (22).

Several enteric pathogens such as *Streptococcus pneumoniae*, *Fusobacterium nucleatum*, *Campylobacter jejuni*, *Listeria monocytogenes* take advantage of disrupted intestinal adherens junctions to internalize in host cells (23-27). How *C. difficile* spores interact with adherens junctions remains poorly described. Herein, we shown that accessible E-cadherin is reduced in differentiated Caco-2 cells. Also, TcdA/TcdB intoxication increases the spore adherence that is correlated with an increase in E-cadherin accessibility in IECs. Next, we observed that *C. difficile* spores interact with E-cadherin in healthy IECs being increased in TcdA/TcdB-intoxicated cells. Also, the blocking of the cellular E-cadherin with monoclonal antibodies reduces the spore adherence and entry to IECs. Finally, we observed that E-cadherin binds to the hair-like extensions of the exosporium.

METHODS

Bacterial growth conditions.

C. difficile R20291 was grown under anaerobic conditions at 37 °C in a Bactron III–2 chamber (Shellab, OR, USA) in BHIS medium; 3.7% brain–heart infusion broth (BD, USA) supplemented with 0.5% of yeast extract (BD, USA), and 0.1% L–cysteine (Merk, USA) liquid or on plates with 1.5% agar (BD, USA). *Bacillus megaterium* transformed with the plasmid pHIS

1522 that contains the cloned genes *tcdA* and *tcdB* of *C. difficile* VPI 10463 (28), were aerobically grown at 37 °C in Luria-Bertani (BD) with 10 µg/mL tetracycline.

Cell lines and culture conditions

Caco-2 cells (ATCC, USA) were grown at 37 °C with 5% CO_2 with Dulbecco's modified Eagle's minimal essential medium High Glucose (DMEM; Hyclone, USA) supplemented with 10% of fetal bovine serum (FBS; Hyclone, USA) and 50 U mL^{-1} penicillin, and 50 µg mL^{-1} streptomycin (Corning Cellgro, USA) as previously has been described For experiments, cells were plated over glass coverslips in 24–well plates and were cultured for 2–days post–confluence (undifferentiated) or 8–days post–confluence (differentiated), changing the media every other day. To polarize Caco-2 cells were cultured onto 12mm Transwell (Corning, USA) with pores size of 0.4 µm until transepithelial electric resistance >250 $\Omega \times cm^2$.

Recombinant *C. difficile* toxin Purification

C. difficile toxins, TcdA and TcdB, were expressed in *B. megaterium* transformed with the plasmid pHIS 1522, containing the cloned genes *tcdA* and *tcdB* of *C. difficile* VPI 10463 as previously described (28). Briefly, transformed *B. megaterium* were cultured in Luria–Bertani medium (BD, USA) supplemented with 10 µg mL^{-1} tetracycline, and 35 mL of an overnight culture was used to inoculate 1L of media. Bacteria were grown at 37 °C with 220 rpm. Toxin expression was induced with 0.5% D–xylose once the culture reached OD_{600} = 0.5. Cells were harvested after 4 h by centrifugation at 4,750×*g* and resuspended in 200 mL of binding buffer (20 mM Tris [pH 8.0], 100 mM NaCl for TcdA and 20 mM Tris [pH 8.0], 500 mM NaCl for TcdB) supplemented with 0.16 µg mL^{-1} DNase, 10 mg mL^{-1} lysozyme and protease inhibitors

(P8849; Sigma). Cell lysis was performed using an Emulsiflex homogenizer, and lysates were centrifuged at 48,000×*g* for 30 min. The toxins were purified from the supernatant by Nickel–affinity, anion exchange, and size–exclusion chromatography. Toxins were eluted and stored in 20 mM HEPES (pH 7.0), 50 mM NaCl.

Spore preparation and purification

C. difficile spores were purified as we previously described (29). Briefly, *C. difficile* spore was cultured overnight in BHI medium in a Bactron III–2 anaerobic chamber (Shellab, USA). Then a 1:500 dilution was plated in TY agar plates; 3% trypticase soy and 0.5% yeast extract and 1.5% Bacto agar (BD, USA) and incubated for 7 days at 37 °C in anaerobiosis. Colonies were harvested with sterile, cold Milli–Q water, washed 3 times and purified with 50% Nicodenz. The spore suspension was 99% free of vegetative cells, sporulating cells, and debris. Spores were quantified in a Neubauer chamber and spores at –80 °C until use.

Immunofluorescence of cell monolayers.

To evaluate E-cadherin distribution in undifferentiated and differentiated Caco-2 cells, cells were washed with PBS and were fixed with PBS–4% paraformaldehyde for 20 min at 4 °C, blocked with PBS–3% BSA 1 h at room temperature (RT). To stain the accessible E-cadherin, cells were incubated with 1: 50 of primary antibody mouse polyclonal anti–human E-cadherin (sc-8426, Santa Cruz Biotechnology, USA) in PBS–3% BSA, for 2 h at RT followed by two washed with PBS and 1:200 secondary antibody donkey anti–mouse-Alexa Fluor 568 (ab175700, Abcam, USA). To detect the total E-cadherin, fixed samples were permeabilized

with PBS-0.2% Triton 100-X for 10 min at RT and blocked with PBS–3% BSA for 1 h at RT. The total protein was detected with the same primary antibody used accessible E-cadherin; primary antibody mouse polyclonal anti–human E-cadherin (sc-8426, Santa Cruz Biotechnology, USA) in PBS–3% BSA that was incubated for 2 h at RT, then were washed and was incubated with 1:200 secondary antibody donkey anti–mouse-Alexa Fluor 568 (ab175700, Abcam, USA). The non–permeabilized samples stained for accessible E-cadherin were permeabilized with PBS-0.2% Triton 100-X for 10 min at RT, washed, and to stain the F–actin, cells were incubated with 1:1,000 Phalloidin i–Fluor 488 (ab176753, Abcam, USA) in PBS for 30 min at RT. Then were washed, and nuclei were stained with 8 µg mL^{-1} Hoechst 33342 (ThermoFisher, USA) in PBS for 10 min at RT. Then samples were washed and mounted using Dako Fluorescent Mounting Medium (Dako, Denmark). Then samples were visualized in the confocal microscope Leica TCS LSI (Leica, Germany). Please see below.

To study the redistribution of E-cadherin in TcdA/TcdB intoxicated cells, differentiated Caco-2 cells cultured into 24–well plates were washed twice with DPBS (Hyclone, USA) and were intoxicated with 600 pM TcdA and 600 pM TcdB for 3, 6, and 8 h in DMEM, without serum. As a control, cells were incubated in the same solution without TcdA/TcdB. Then cells were rinsed with PBS, fixed with PBS–4% paraformaldehyde, and washed with PBS and blocked with PBS–1% BSA at 4 °C overnight. To stain the surface, accessible E-cadherin cells were incubated with 1:200 mouse mAb anti–E-cadherin (SC8426, Santa Cruz Biotechnologies, USA), 1 h at RT, washed, and followed incubation with 1:400 donkey anti–mouse IgG Alexa Fluor 488 (ab150109, Abcam, USA) for 1 h at RT. To detect the total protein, samples were permeabilized with PBS–0.2% Triton 100-X for 10 min at RT and blocked with PBS–1% BSA

for 1 h at RT. The total protein was detected with the same primary antibody used before, washed, and were incubated with donkey anti–mouse IgG Alexa Fluor 568 (ab175700, Abcam, USA). Samples were mounted using Dako Fluorescent Mounting Medium (Dako, Denmark) and were visualized in the confocal microscope Leica Sp8 (Leica, Germany; please see below.)

To evaluate *C. difficile* spore association with accessible E-cadherin in TcdA/TcdB intoxicated IECs, differentiated Caco-2 cells were intoxicated with 600 pM TcdA and 600 pM TcdB for 8 h at RT, as is describes above. Then cells were infected with *C. difficile* spores in an MOI of 10 for 1 h at 37 °C. Then cells were washed, fixed with PBS–4% paraformaldehyde for 10 min at RT, blocked with PBS–1% BSA overnight at 4 °C, and *C. difficile* spores were stained with 1:1,000 primary polyclonal anti–*C. difficile* spore IgY batch 7246 antibodies (30) (Aveslab, USA) in PBS–1% BSA for 1 h at RT. Following two PBS washed, samples were incubated with 1:400 goat anti–chicken IgY secondary antibodies Alexa–Fluor 488 (#ab150173 Abcam, USA) in PBS–3% BSA for 1 h at RT, washed two times with PBS, and accessible E–cadherin was stained as is described above. Cellular nuclei was stained with 8 µg mL^{-1} Hoechst 33342 (ThermoFisher, USA) for 15 min at RT. Finally, samples were mounted and analyzed by confocal microscopy Leica SP8.

The Leica microscopes TCS LSI and SP8 at the Confocal Microscopy Core Facility of the Universidad Andrés Bello were used. To evaluate E-cadherin distribution in undifferentiated and differentiated Caco-2 cells, Leica TCS LSI was used with 63× ACS APO oil objective numerical aperture 1.3, with an optical zoom of 2×. Micrographs were acquired using excitation wavelengths of 405, 488, and 532 nm, and signals were detected with an ultra–high dynamic

photomultiplier (PMT) spectral detector (430–750nm). Emitted fluorescence was split with four dichroic mirrors (QD 405, 488, 561, and 635 nm). Images 1,024 × 1,024 pixels were acquired each 0.3 µm. To observe the redistribution of accessible E-cadherin and total E-cadherin in TcdA and TcdB intoxicated cells, Leica SP8 was used with HPL APO CS2 40× oil, numerical aperture 1.30. For signal detection, three PMT spectral detectors were used; PMT1 (410–483) DAPI, PMT2 (505–550), Alexa–Fluor 488, and PMT3 (587–726) Alexa–Fluor 555. Emitted fluorescence was split with dichroic mirrors DD488/552. Pictures of 1,024 × 1,024 pixels were captured each 0.3 µm. Images of 3–dimensional reconstructions of the Caco-2 monolayers were performed using ImageJ software (NIH, USA). In undifferentiated and differentiated cells, accessible E-cadherin cells were quantified as the number of cells with positives staining. To quantify the redistribution of E-cadherin, Fl. Int. of each slide was measured using the plug–in "Measure stack" of Fiji (ImageJ, NHI, USA) and the sum of the Fl. Int. of each slide is considered as the Fl. Int. of the *z*–stack of a field for accessible and total E-cadherin. For each field, the same number of slides was used.

Quantification of *C. difficile* spore adherence and internalization.

To evaluate spore adherence and internalization in TcdA/TcdB intoxicated cells, differentiated Caco-2 cells were incubated with 600 pM TcdA and 600 pM TcdB for 3, 6, and 8 h in DMEM, without serum. As a control, cells were incubated in the same solution without TcdA/TcdB. Then cells were infected with *C. difficile* spores an MOI 10 for 3 h at 37 °C. Unbound spores were rinsed off with PBS, and cells were fixed with PBS–4% paraformaldehyde for 10 min, and adhered spores were stained as is described below.

To evaluate spore adherence and entry in presence of anti–E-cadherin, undifferentiated, differentiated, and polarized Caco-2 cells were incubated with 0,1; 1,0; 10; 100 µg mL^{-1} of mouse monoclonal anti–human E-cadherin (SC8426, Santa Cruz Biotechnology, USA) or as control non–immune IgG antibody of rabbit serum (I5006, Sigma-Aldrich, USA) for 2 h at 37 °C. Then cells were infected for 3 h at 37 °C with *C. difficile* spores, previously incubated with 20 µL of FBS per well for 1 h at 37 °C. Cells were washed two times with PBS to remove unbound spores and were fixed with PBS–4% paraformaldehyde for 10 min at RT, and adhered spores were stained as is described as follows.

In undifferentiated, differentiated, and polarized *C. difficile* spore infected Caco-2 cells, adhered *C. difficile* spores were immunostained using the intracellular spore exclusion immunostaining assay as previously described (20). For this *C. difficile* spore–infected cells were washed three times with PBS at RT and were blocked with PBS–3% BSA overnight at 4 °C, and samples were incubated with anti–*C. difficile* spore goat serum 1:50 (PAC 5573, Pacific Immunology, USA) in PBS–1% BSA for 1 h at RT. Then were washed 3 times with PBS and were incubated with 1:400 secondary antibody donkey IgG anti–goat CFL 488 (SC362255, Santa Cruz Biotechnology, USA) for 1 h at RT. Cells were washed, and DNA was stained with 8 µg mL^{-1} Hoechst 33342 (ThermoFisher, USA) for 15 min at RT. In the case of polarized cells, to stain the F–actin, samples were incubated with 1:100 Phalloidin Alexa Fluor 568 (A12380, Invitrogen, USA) for 30 min at RT. Samples were washed three times with PBS and one time with distilled water and mounted with Dako Fluorescent Mounting Medium (Dako, Denmark). Samples were visualized in the epifluorescence microscope Olympus BX53 fluorescence microscopy with UPLFLN 100× oil objective (numerical aperture 1.30). Images were captured

with the camera for fluorescence imaging Qimaging R6 Retiga and pictures were analyzed with ImageJ (NIH, USA). Adhered spores were considered as spores in phase–contrast that were marked in fluorescence. Internalized spores were considered spores in phase–contrast, but that does not have fluorescence. In the case of polarized cells, only was possible to quantify adhered spores. Number or adhered spores were quantified, and data were relativized to the control.

ELISA of E-cadherin bound to *C. difficile* spores.

1.6×10^8 *C. difficile* spores or 1 µg of BSA as control were incubated in wells of a 96–wells plate in PBS overnight at 4 °C. Wells were washed 5 times with PBS–0.05% Tween-20 (PBS–Tween) to remove unbound spores, and wells were blocked with 200 µL of PBS–Tween–2% BSA (Sigma Aldrich, USA) for 1 h at 37 °C. Then were washed and incubated with 50 µL of at 0.2, 2.0, 20, and 200 nM of recombinant human purified E-cadherin (5085, Sigma-Aldrich, USA) for 1 h at 37 °C. Unbonded E-cadherin was washed 5 times with PBS–Tween and was incubated with 50 µL of 1:50 IgG of mouse anti–E-cadherin (SC8426-Santa Cruz Biotechnology, USA) in PBS–Tween–1% BSA for 1 h at 37 °C. Wells were washed five times with PBS–Tween and then incubated with 50 µL of 1: 5,000 secondary antibody anti–mouse-HRP (610-1302, Rockland, USA) 1 h at 37 °C. Then, wells were washed five times with PBS–Tween and once with carbonate buffer (pH 9.6). Finally, wells were incubated with 50 µL of buffer substrate (17 mM citric acid, 65 mM potassium phosphate, 0.15% hydrogen peroxide, and 0.4% θ-phenylenediamine) for 20 min at RT. The reaction was stopped with 25µL of 4.5 N H_2SO_4. The color intensity was quantified at 450nm using the plate reader Infinite F50, (Tecan, Switzerland).

Immunofluorescence of E-cadherin bound to *C. difficile* spores.

The immunofluorescence was performed as previously have been described with modification (19). Briefly, 4×10^7 *C. difficile* spores, were incubated with 1, 2.5, 5.0, 10, and 25 µg mL^{-1} of recombinant human purified E-cadherin (5085, Sigma-Aldrich, USA) in PBS for 1 h at 37 °C. Spores were washed 5 times with PBS and were fixed with PBS–4% paraformaldehyde in poly–L-lysine-treated 12mm glass–coverslips (Marienfeld GmbH, Germany). Then were washed 3 times with PBS and were blocked with PBS–3% BSA for 1 h at RT. Furthermore, samples were incubated with 1:50 mouse IgG anti–E-cadherin (SC8426, Santa Cruz Biotechnology, USA) for 2 h at RT and then washed 3 times with PBS and once with distilled H_2O. Finally, samples were mounted with Dako Fluorescent Mounting Medium (Dako, Denmark), and images were captured in an epifluorescence microscope Olympus BX53. The fluorescence intensity was quantified using Fiji (ImageJ, NHI, USA). Data were normalized as $(\text{Fl. Int/area})_{\text{sample}} - (\text{Fl. Int/area})_{\text{background}}$. The Surface Plot was generated with the plug–in 3D surface Plot of Fiji (ImageJ, NHI, USA).

Transmission electron microscopy of E-cadherin bound to *C. difficile* spores.

2.5×10^8 *C. difficile* spores were incubated with 10 µg mL^{-1} of recombinant human purified E-cadherin (5085, Sigma-Aldrich, USA) with PBS for 1 h at 37 °C. Spores were washed 5 times with PBS and centrifugation at 18,400×*g* for 5 min and were blocked with PBS–1% BSA for 20 min at RT. Then samples were incubated with 1:50 IgG of mouse anti–E-cadherin (SC8426, Santa Cruz Biotechnologies, USA) in PBS–1% BSA for 1 h at RT, washed 3 times by centrifugation at 18,400×*g* for 5 min with PBS. Spores were incubated with IgG anti–mouse conjugated to 10nm gold nanoparticles (G7777, Sigma-Aldrich, USA) for 1 h at RT. Then were

washed 3 times with PBS–0.1% BSA by centrifugation at 18,400×*g* for 5 min. Subsequently, spores were processes for TEM, as previously have been described (19). Briefly, spores were fixed in 0.1 M cacodylate buffer–2.5% glutaraldehyde with 1% paraformaldehyde and then fixed with 0.1 M cacodylate buffer–1% osmium tetroxide and stained with 1% tannic acid for 30 min. Samples were dehydrated with increasing acetone concentrations; 30% acetone (with 2% uranyl acetate only in this step) for 30 min, 50% acetone for 30 min, 70% acetone overnight, and 90% acetone for 30 min, and 2 times with 100% acetone. Dehydrated samples were embedded in resin: acetone in a ratio of 3:1, 1:1, and 1: 3 for 40 min each. Finally, samples were resuspended in resin for 4 h and incubated for 12 h at 65 °C. With a microtome, 90 nm sections cut and placed in a carbon–coated grid for negative staining and double staining with 2% uranyl acetate with lead citrate. Sections were observed in a transmission electron microscope Phillip Tecnai 12 bioTwin of the Pontificia Universidad Católica de Chile. The distribution of thin or thick exosporium was quantified according to previously described morphotypes (31).

RESULTS

Characterization of accessible E-cadherin in monolayers of Caco-2 cells. Caco-2 cells have been employed to assess *C. difficile* interaction with IECs (18-20, 29, 30, 32-34). Early work demonstrated that *C. difficile* spores had a tropism towards the cell-cell junction of EDTA-treated Caco-2 cells (18). Therefore, to understand the dynamic of adherens junction closure during Caco-2 cells differentiation, we assessed the accessibility of E-cadherin in undifferentiated and differentiated monolayers of Caco-2 cells. First, Caco-2 cell differentiation was assessed for the appearance of microvilli by TEM and sucrase-isomaltose as a differentiation

marker in monolayers cultured for 2- or 8-days post-confluency (19). Next, differentiated and undifferentiated Caco-2 cells were immunostained for accessible E-cadherin or permeabilized and stained for total E-cadherin (Figure 1*A, B*). Results demonstrate that in undifferentiated Caco-2 cells, ~84% of the cells were immunolabeled for accessible E-cadherin (Figure 1*C*), whereas, in differentiated Caco-2 cells, only ~7% of the cells were stained for accessible E-cadherin (Figure 1*C*). As control, cells were permeabilized and stained for total E-cadherin, and we observed that ~100% of both undifferentiated and differentiated Caco-2 cells were immunolabeled for E-cadherin (Figure 1*D-F*). These results demonstrate that after 8-days of differentiation, most of the cells lack accessible E-cadherin.

Intoxication with *C. difficile* TcdA and TcdB increases accessible E-cadherin. *C. difficile* toxins TcdA and TcdB cause tight and adherens junctions dissociation (9-11). TcdA, but not TcdB, cause a displacement of E-cadherin from the cell-cell junctions to be located around the cells in Caco-2 cells (11) while in colonic epithelium, TcdB causes adherens junctions disruption (10). We asked whether the TcdA and TcdB affect the accessibility of E-cadherin in differentiated Caco-2 cells. TcdA/TcdB-intoxicated differentiated Caco-2 cells for 3, 6, and 8h were immunostained for accessible E-cadherin (non-permeabilized) using an antibody that detects an extracellular domain of E-cadherin, followed by fluorescent-labeled secondary antibody. For total E-cadherin staining, cells were permeabilized and immunostained with the same primary antibody and a fluorescent-labeled secondary antibody with another Alexa Fluor dye (See Methods). Then, we acquired confocal micrographs, and the fluorescence intensity (Fl. Int.) was quantified for every slice of the *z*-stack for accessible and total E-cadherin. The sum of the Fl. Int. of accessible E-cadherin was significantly higher (175% relative to unintoxicated

monolayers) after 8h-intoxication (Figure 2*A, B,* Supplementary Figure 1). To evaluate if this increase of Fl. Int. occurs in the apical or basal half of the monolayer, we split the number of slices of the z-stack into 2-halves (apical and basal) with the same number of slices. We summed the Fl. Int. for accessible E-cadherin in the apical (Figure 2*C*) or basal (Figure 2*D*) halves of the monolayer. We observed a significant increase in accessible E-cadherin Fl.Int. in 177% and 176% in the apical and basal halves, respectively, after 8h-intoxication (Figure 2*C, D*). Using the same strategy, we quantified the total E-cadherin Fl. Int. in the complete *z*-stack, and we observed a significant decrease of 19% after 6h- and an increase of 12.2% after 8h-intoxication compared to unintoxicated cells (Figure 2*E*). Then, we observed that these variations were in the apical and not in the basal half of the monolayer. We observed a decrease of 35% after 6h- and an increase of 44% after 8h-intoxication compared to unintoxicated cells (Figure 2*F, G*). Consequently, these results indicate that accessible E-cadherin is increased in differentiated Caco-2 cells after 8h-intoxication.

***C. difficile* toxins TcdA and TcdB increase the adherence to IECs.** Several studies shown that vegetative *C. difficile*-adherence to IECs is enhanced following TcdA or CDT intoxication (11, 35, 36). To expand the impact of intoxication of IECs on spore-adherence, TcdA/TcdB 8h-intoxicated differentiated Caco-2 cells were infected for 3h with *C. difficile* spores in absence of serum. Then cells were fixed, and without permeabilization, adhered spores immunostained. In TcdA/TcdB intoxicated Caco-2 cells, we observed more adhered spores compared to unintoxicated cells (Figure 3*A-B*). After quantitative analysis, we observed that spore adherence in 8h-TcdA/TcdB-intoxicated cells was 170% higher than in unintoxicated monolayers (Figure 3*C*). We recently demonstrated that *C. difficile* spores gain entry into IECs in the presence of

fibronectin, vitronectin, or serum (20). Therefore, we assessed whether TcdA/TcdB intoxication affects spore entry into IECs in absence of these proteins. To identify intracellular spores, we used the intracellular spore exclusion immunostaining assay previously described (20), where only extracellular spores are immunostained in non-permeabilized cells, and total spores are visualized by phase-contrast microscopy. Using this strategy, we observed that the percentage of internalized spores (visualized in phase-contrast but not in fluorescence) was ~0.2%, both in intoxicated and unintoxicated Caco-2 cells (Figure 3*D*). Collectively, these data indicate that TcdA/TcdB-intoxication of differentiated Caco-2 cells increases *C. difficile* spore adherence but not internalization.

Intoxication of IECs increases *C. difficile* spore association with E-cadherin. Since we observed that TcdA/TcdB-intoxicated differentiated Caco-2 cells lead to an increase of accessible E-cadherin and adherence of *C. difficile* spores, we tested whether this could be attributed to *C. difficile* spores associating with accessible E-cadherin. For this, unintoxicated or TcdA/TcdB-intoxicated differentiated Caco-2 cells were infected with *C. difficile* spores for 1h. Then, accessible E-cadherin and spores were immunostained and visualized by confocal microscopy (Figure 4*A, D*). Plot profile analysis of unintoxicated Caco-2 cells (Figure 4*A*) reveals that ~21% of adhered *C. difficile* spores were associate with accessible E-cadherin (Figure 4*B, C,* and *G*). Notably, upon TcdA/TcdB-intoxication (Figure 4*D*), ~72% of adhered spores were associated with accessible E-cadherin (Figure 4*E, F, G*). These results indicate that adhered *C. difficile* spores can associate with accessible E-cadherin in IECs, and this association is enhanced upon TcdA/TcdB-intoxication.

Antibody blocking of accessible E-cadherin reduces adherence and internalization of *C. difficile* spores to IECs. Next, we assessed whether E-cadherin is involved in *C. difficile* spore adherence and internalization. We have shown that *C. difficile* spore internalization occurs in serum presence (20). Therefore, undifferentiated, differentiated, and polarized Caco-2 cells were incubated with anti-E-cadherin for 2h and subsequently infected for 3h with FBS-incubated *C. difficile* spores. Afterward, we quantified *C. difficile* spore adherence and internalization using the intracellular spore exclusion immunostaining assay. In undifferentiated Caco-2 cells, we observed that *C. difficile* spore adherence to IECs was significantly decreased upon increasing concentrations of anti-E-cadherin; spore adherence decreased by 38, 53, and 73% compared to the control when cells were incubated with 1, 10, and 100 µg/mL of anti-E-cadherin, respectively (Figure 5*A*). Upon quantifying internalization in undifferentiated Caco-2 cells, we observed a significant decrease of 38, 43, and 69% compared to the control in cells incubated with 1, 1, 100 µg/mL of anti-E-cadherin, respectively (Figure 5*B*). Similarly, in differentiated Caco-2 cells, a significant decrease in spore adherence in 18, 32, 60, and 70% compared to the control was observed in cells incubated with 0.1, 1, 10, and 100 µg/mL of anti-E-cadherin, respectively (Figure 5*C*). For internalization, we observed a significant decrease in 15, 35, 42, and 54% compared to the control in cells incubated with 0.1, 1, 10, and 100 µg/mL of anti-E-cadherin, respectively (Figure 5*D*). Finally, in polarized Caco-2 cells, we observed a decrease in 32, 56, 63, and 79% in spore adherence compared to the control in presence with 0.1, 1, 1,0, and 100 µg/mL of anti-E-cadherin, respectively (Figure 5*E*). These data indicate that the antibody-mediated blockage of accessible E-cadherin reduces *C. difficile* spore adherence and internalization to IECs.

E-cadherin binds in concentration-dependent manner to *C. difficile* spores. To provide evidence that *C. difficile* spores interact with E-cadherin, we used ELISA with *C. difficile* spore-coated wells incubated with increasing concentrations of E-cadherin, or BSA as control. E-cadherin binding activity was evident in *C. difficile* spore-coated wells (Fig. 6*A*). The specificity of this interaction was demonstrated by the dose-dependent binding. Additionally, we evaluated the distribution of binding of E-cadherin to the spore surface by immunofluorescence. Upon micrograph analysis, we observed that anti-E-cadherin immunostained spores exhibited a non-homogeneous Fl. Int surrounding the spore (Fig. 6*B*). In spores, the Fl. Int. for E-cadherin was 156, 189, 258, 304, and 369% relative to the control upon incubation with 1, 2.5, 5, 10, and 25 µg/mL of E-cadherin (Fig. 6*C*). Next, we established a Fl. Int cut-off limit for those *C. difficile* spores that were visually associated with 2.5 µg/mL E-cadherin. Based on this threshold, 59, 65, and 66% of the spores were positive for E-cadherin in the presence of 5, 10, and 25 µg/mL E-cadherin, respectively. Then, we evaluated E-cadherin Fl. Int distribution for positive immunodetected spores, and we observed that were mainly distributed between 1.4-2.1 normalized Fl. Int. arbitrary units. (Fig. 6*D*). Overall, these results suggest that E-cadherin interacts with *C. difficile* spores in a dose-dependent manner and that E-cadherin-ligand binding sites are non-homogeneous distributed on the *C. difficile* spore surface.

E-cadherin interacts with hair-like projections of *C. difficile* spores. The outermost structure of *C. difficile* spores are the hair-like projections that are common in epidemically relevant strains (16), and that BclA3 is required for its correct formation (20). In addition, isogenic sporulating cultures of *C. difficile* lead to the formation of spores with two exosporium morphotypes that exhibit hair-like projections, spores with a thick exosporium layer exhibits

distinctive electron-dense bumps, and spores with a thin electron-dense layer (31, 37, 38). Consequently, to gain ultrastructural insight of spore-E-cadherin interaction, we used TEM of immunogold-labeling E-cadherin of *C. difficile* spores. We observed E-cadherin-gold particles in close contact with the exosporium of *C. difficile* spores, particularly with hair-like projection (Figure 7*A-E*). No gold particles were observed in spores without E-cadherin. (Figure 7*A*). We observed gold particles in 52/236 (22.1%) of the spores (Figure 7*F*). Of which, 19/52 (36.5%) and 33/52 (63.5%) spores correspond to spores with thin and thick exosporium, respectively (Figure 7*G*). Nevertheless, due to sample preparation, we only visualized a 90nm-slide of the sample, implicating that the number of gold particles is for one slice and not to the complete spore. These results suggest that E-cadherin binds preferentially to thick-exosporium layer spores and specifically to the hair-like projections.

DISCUSSION

The integrity of the intestinal epithelial barrier is key in preventing pathogen translocation (22). In the healthy intestinal mucosa, the apical- and basolateral-cell side are not completely sealed, in which E-cadherin is accessible, i.e., along lateral membranes of goblet cells (20, 39, 40), extruding apoptotic sites, produced transiently when senescent cells are expelled and detached from the epithelium (39, 41, 42) and in epithelial folds of the intestinal villus produced by tension and constriction forces (39). *C. difficile* spores are regarded as a key virulence factor required for survival of *C. difficile* in the environment and transmission of the disease (16, 17). Recent evidence of how *C. difficile* spore interacts with the intestinal barrier has suggested that spores employ extracellular matrix proteins, as molecular bridging molecules to interact with integrin receptors and gain intracellular access to IECs (19, 20). Notably, these molecular bridging molecules and integrin receptors are typically located in the basolateral membrane (36, 43-46), consistent with early observations in EDTA–treated differentiated monolayers of Caco-2 cells where spores have a tropism for the cell–cell junction of IECs (18). In this work, we expanded our understanding of how *C. difficile* spores adhere to IECs by showing that *C. difficile* spores exhibit tropism to the adherens junctions protein E-cadherin, consistent with early observations in EDTA-treated differentiated Caco-2 cells where spores have a tropism for the cell-cell junction (18).

A main conclusion of this work is that *C. difficile* spores adhered to IECs, associate with accessible human E-cadherin, and blockage of this association lead to reduced *C. difficile* spore adherence and entry. Recently we demonstrated that *C. difficile* spores gain entry into IECs through fibronectin- and vitronectin-integrin-dependent pathways (20). Notably, these molecules

are located in the basolateral membrane (36, 43-45). Results from this work suggest that *C. difficile* spores might take advantage of accessible E-cadherin to facilitate binding and subsequent internalization through the fibronectin- and vitronectin-dependent pathways (19, 20). This strategy is commonly employed by enteric pathogens, among which *L. monocytogenes* is well studied (26, 47, 48). Since E-cadherin is not extensively accessible in the intestinal mucosa, *L. monocytogenes* internalize through goblets cells, extrusion sites, or epithelial folds (39, 49).

Another major conclusion of this work is that *C. difficile* spores bind to E-cadherin in a dose-dependent manner and apparently through the hair-like projections of the exosporium. *L. monocytogenes* interacts with humans and not with mouse E-cadherin through InlA (26). However, the exosporium of *C. difficile* spores has no orthologs of InlA (50). We recently demonstrated that BclA3 is implicated in the formation of the hair-like projections and interacts with fibronectin and vitronectin (20), and spore mutants in BclA3 showed a reduces entry but not adherence *in vitro* in the presence of fibronectin and vitronectin, and *in vivo* showed reduced adherence but not entry in the intestinal mucosa (20). Therefore, the hair-like projections might be a potential target to reduce the interaction of *C. difficile* spores with the intestinal mucosa (20). Current ongoing work in our laboratory aims to address the interaction of the hair–like projections with *C. difficile* spores and whether additional spore proteins are implicated.

C. difficile toxins TcdA and TcdB cause a disruption of the cell-cell junctions (10, 12, 13), causing loss of cellular polarity (9-11) due, dissociation of tight and adherens junctions proteins. In this context, our work contributes to understanding how *C. difficile* spores interact with TcdA/TcdB-intoxicated IECs. Our results demonstrate that differentiated TcdA/TcdB-

intoxicated monolayers showed increased accessibility of E-cadherin that correlated with an increase in the *C. difficile* spore adherence to TcdA/TcdB-intoxicated cells. Also, in a healthy epithelium, we observed a small fraction of *C. difficile* spores associated with E-cadherin, but this association is enhanced in intoxicated differentiated Caco-2 cells.

Recently, we reported that *C. difficile* spore entry contributes to the R-CDI. In particular, we observed that nystatin inhibits the spore entry and reduces R-CDI in a mouse model (20). The increase in the spore adherence in TcdA/TcdB-intoxicated cells, coupled to the inhibition of *C. difficile* spore adherence and entry with anti-E-cadherin, suggest that during CDI, TcdA, and TcdB increase the E-cadherin accessibility, contributing to the spore adherence and entry. This could explain the observations of clinical studies with CDI patients where the presence of high titers of endogenous antibodies against TcdB, but not TcdA, correlated with reduced R-CDI rates (51). Consistently, bezlotoxumab administration combined with antibiotics reduces the R-CDI rates (15). Consequently, the development of multifactorial treatment with intervention in TcdA/TcdB, spore adherence, and entry to IECs might importantly reduce the R-CDI rates.

NOTES

CONFLICT OF INTEREST. The authors declare that they have no conflict of interest.

FUNDING. This work was funded by FONDECYT Regular 1191601, and by Millennium Science Initiative Program - NCN17_093, and Startup funds from the Department of Biology at Texas A&M University to D.P-S. Additional funding support to P.C-C from ANID-PCHA/Doctorado Nacional/ 2016-21161395.

REFERENCES

1. Redelings MD, Sorvillo F, Mascola L. 2007. Increase in *Clostridium difficile*-related mortality rates, United States, 1999-2004. Emerg Infect Dis 13:1417-9.
2. Stevens VW, Nelson RE, Schwab-Daugherty EM, Khader K, Jones MM, Brown KA, Greene T, Croft LD, Neuhauser M, Glassman P, Goetz MB, Samore MH, Rubin MA. 2017. Comparative Effectiveness of Vancomycin and Metronidazole for the Prevention of Recurrence and Death in Patients With *Clostridium difficile* Infection. JAMA Intern Med 177:546-553.
3. Di X, Bai N, Zhang X, Liu B, Ni W, Wang J, Wang K, Liang B, Liu Y, Wang R. 2015. A meta-analysis of metronidazole and vancomycin for the treatment of *Clostridium difficile* infection, stratified by disease severity. Braz J Infect Dis 19:339-49.
4. Lyerly DM, Lockwood DE, Richardson SH, Wilkins TD. 1982. Biological activities of toxins A and B of *Clostridium difficile*. Infect Immun 35:1147-50.
5. Lyras D, O'Connor JR, Howarth PM, Sambol SP, Carter GP, Phumoonna T, Poon R, Adams V, Vedantam G, Johnson S, Gerding DN, Rood JI. 2009. Toxin B is essential for virulence of *Clostridium difficile*. Nature 458:1176-9.
6. Kuehne SA, Cartman ST, Heap JT, Kelly ML, Cockayne A, Minton NP. 2010. The role of toxin A and toxin B in *Clostridium difficile* infection. Nature 467:711-3.
7. Just I, Selzer J, Wilm M, von Eichel-Streiber C, Mann M, Aktories K. 1995. Glucosylation of Rho proteins by *Clostridium difficile* toxin B. Nature 375:500-3.
8. Just I, Wilm M, Selzer J, Rex G, von Eichel-Streiber C, Mann M, Aktories K. 1995. The enterotoxin from *Clostridium difficile* (ToxA) monoglucosylates the Rho proteins. J Biol Chem 270:13932-6.
9. Nusrat A, von Eichel-Streiber C, Turner JR, Verkade P, Madara JL, Parkos CA. 2001. *Clostridium difficile* toxins disrupt epithelial barrier function by altering membrane microdomain localization of tight junction proteins. Infect Immun 69:1329-36.
10. Mileto SJ, Jardé T, Childress KO, Jensen JL, Rogers AP, Kerr G, Hutton ML, Sheedlo MJ, Bloch SC, Shupe JA, Horvay K, Flores T, Engel R, Wilkins S, McMurrick PJ, Lacy DB, Abud HE, Lyras D. 2020. *Clostridioides difficile* infection damages colonic stem cells via TcdB, impairing epithelial repair and recovery from disease. Proc Natl Acad Sci U S A 117:8064-8073.
11. Kasendra M, Barrile R, Leuzzi R, Soriani M. 2014. *Clostridium difficile* toxins facilitate bacterial colonization by modulating the fence and gate function of colonic epithelium. J Infect Dis 209:1095-104.
12. Hecht G, Pothoulakis C, LaMont JT, Madara JL. 1988. *Clostridium difficile* toxin A perturbs cytoskeletal structure and tight junction permeability of cultured human intestinal epithelial monolayers. J Clin Invest 82:1516-24.
13. Hecht G, Koutsouris A, Pothoulakis C, LaMont JT, Madara JL. 1992. *Clostridium difficile* toxin B disrupts the barrier function of T84 monolayers. Gastroenterology 102:416-23.
14. Leslie JL, Huang S, Opp JS, Nagy MS, Kobayashi M, Young VB, Spence JR. 2015. Persistence and toxin production by *Clostridium difficile* within human intestinal

532 organoids result in disruption of epithelial paracellular barrier function. Infect Immun
533 83:138-45.
534 15. Wilcox MH, Gerding DN, Poxton IR, Kelly C, Nathan R, Birch T, Cornely OA, Rahav G,
535 Bouza E, Lee C, Jenkin G, Jensen W, Kim YS, Yoshida J, Gabryelski L, Pedley A, Eves K,
536 Tipping R, Guris D, Kartsonis N, Dorr MB, Investigators MIaMI. 2017. Bezlotoxumab for
537 Prevention of Recurrent *Clostridium difficile* Infection. N Engl J Med 376:305-317.
538 16. Paredes-Sabja D, Shen A, Sorg JA. 2014. *Clostridium difficile* spore biology: sporulation,
539 germination, and spore structural proteins. Trends Microbiol 22:406-16.
540 17. Deakin LJ, Clare S, Fagan RP, Dawson LF, Pickard DJ, West MR, Wren BW, Fairweather
541 NF, Dougan G, Lawley TD. 2012. The *Clostridium difficile spo0A* gene is a persistence and
542 transmission factor. Infect Immun 80:2704-11.
543 18. Paredes-Sabja D, Sarker MR. 2012. Adherence of *Clostridium difficile* spores to Caco-2
544 cells in culture. J Med Microbiol 61:1208-1218.
545 19. Mora-Uribe P, Miranda-Cardenas C, Castro-Cordova P, Gil F, Calderon I, Fuentes JA,
546 Rodas PI, Banawas S, Sarker MR, Paredes-Sabja D. 2016. Characterization of the
547 Adherence of *Clostridium difficile* Spores: The Integrity of the Outermost Layer Affects
548 Adherence Properties of Spores of the Epidemic Strain R20291 to Components of the
549 Intestinal Mucosa. Front Cell Infect Microbiol 6:99.
550 20. Castro-Córdova P, Mora-Uribe P, Reyes-Ramírez R, Cofré-Araneda G, Orozco-Aguilar J,
551 Brito-Silva C, Mendoza-León MJ, Kuehne SA, Minton NP, Pizarro-Guajardo M, Paredes-
552 Sabja D. 2021. Entry of spores into intestinal epithelial cells contributes to recurrence of
553 *Clostridioides difficile* infection. Nat Commun 12:1140.
554 21. Buckley A, Turner JR. 2018. Cell Biology of Tight Junction Barrier Regulation and Mucosal
555 Disease. Cold Spring Harb Perspect Biol 10.
556 22. Paradis T, Bègue H, Basmaciyan L, Dalle F, Bon F. 2021. Tight Junctions as a Key for
557 Pathogens Invasion in Intestinal Epithelial Cells. Int J Mol Sci 22.
558 23. Rubinstein MR, Wang X, Liu W, Hao Y, Cai G, Han YW. 2013. *Fusobacterium nucleatum*
559 promotes colorectal carcinogenesis by modulating E-cadherin/β-catenin signaling via its
560 FadA adhesin. Cell Host Microbe 14:195-206.
561 24. Anderton JM, Rajam G, Romero-Steiner S, Summer S, Kowalczyk AP, Carlone GM,
562 Sampson JS, Ades EW. 2007. E-cadherin is a receptor for the common protein
563 pneumococcal surface adhesin A (PsaA) of *Streptococcus pneumoniae*. Microb Pathog
564 42:225-36.
565 25. Elmi A, Nasher F, Jagatia H, Gundogdu O, Bajaj-Elliott M, Wren B, Dorrell N. 2016.
566 *Campylobacter jejuni* outer membrane vesicle-associated proteolytic activity promotes
567 bacterial invasion by mediating cleavage of intestinal epithelial cell E-cadherin and
568 occludin. Cell Microbiol 18:561-72.
569 26. Mengaud J, Ohayon H, Gounon P, Mege R-M, Cossart P. 1996. E-cadherin is the receptor
570 for internalin, a surface protein required for entry of *L. monocytogenes* into epithelial
571 cells. Cell 84:923-32.
572 27. Ribet D, Cossart P. 2015. How bacterial pathogens colonize their hosts and invade
573 deeper tissues. Microbes Infect 17:173-83.
574 28. Chandrasekaran R, Kenworthy AK, Lacy DB. 2016. *Clostridium difficile* Toxin A Undergoes
575 Clathrin-Independent, PACSIN2-Dependent Endocytosis. PLoS Pathog 12:e1006070.

576 29. Calderon-Romero P, Castro-Cordova P, Reyes-Ramirez R, Milano-Cespedes M, Guerrero-
577 Araya E, Pizarro-Guajardo M, Olguin-Araneda V, Gil F, Paredes-Sabja D. 2018.
578 *Clostridium difficile* exosporium cysteine-rich proteins are essential for the
579 morphogenesis of the exosporium layer, spore resistance, and affect *C. difficile*
580 pathogenesis. PLoS Pathog 14:e1007199.
581 30. Pizarro-Guajardo M, Diaz-Gonzalez F, Alvarez-Lobos M, Paredes-Sabja D. 2017.
582 Characterization of Chicken IgY Specific to *Clostridium difficile* R20291 Spores and the
583 Effect of Oral Administration in Mouse Models of Initiation and Recurrent Disease. Front
584 Cell Infect Microbiol 7:365.
585 31. Pizarro-Guajardo M, Calderon-Romero P, Castro-Cordova P, Mora-Uribe P, Paredes-
586 Sabja D. 2016. Ultrastructural Variability of the Exosporium Layer of *Clostridium difficile*
587 Spores. Appl Environ Microbiol 82:2202-2209.
588 32. Schöttelndreier D, Langejürgen A, Lindner R, Genth H. 2020. Low Density Lipoprotein
589 Receptor-Related Protein-1 (LRP1) Is Involved in the Uptake of *Clostridioides difficile*
590 Toxin A and Serves as an Internalizing Receptor. Front Cell Infect Microbiol 10:565465.
591 33. Tam J, Icho S, Utama E, Orrell KE, Gómez-Biagi RF, Theriot CM, Kroh HK, Rutherford SA,
592 Lacy DB, Melnyk RA. 2020. Intestinal bile acids directly modulate the structure and
593 function of *C.difficile* TcdB toxin. Proc Natl Acad Sci U S A 117:6792-6800.
594 34. Landenberger M, Nieland J, Roeder M, Nørgaard K, Papatheodorou P, Ernst K, Barth H.
595 2021. The cytotoxic effect of *Clostridioides difficile* pore-forming toxin CDTb. Biochim
596 Biophys Acta Biomembr 1863:183603.
597 35. Schwan C, Stecher B, Tzivelekidis T, van Ham M, Rohde M, Hardt WD, Wehland J,
598 Aktories K. 2009. *Clostridium difficile* toxin CDT induces formation of microtubule-based
599 protrusions and increases adherence of bacteria. PLoS Pathog 5:e1000626.
600 36. Schwan C, Kruppke AS, Nolke T, Schumacher L, Koch-Nolte F, Kudryashev M, Stahlberg
601 H, Aktories K. 2014. *Clostridium difficile* toxin CDT hijacks microtubule organization and
602 reroutes vesicle traffic to increase pathogen adherence. Proc Natl Acad Sci U S A
603 111:2313-8.
604 37. Pizarro-Guajardo M, Calderon-Romero P, Paredes-Sabja D. 2016. Ultrastructure
605 Variability of the Exosporium Layer of *Clostridium difficile* Spores from Sporulating
606 Cultures and Biofilms. Appl Environ Microbiol 82:5892-8.
607 38. Pizarro-Guajardo M, Calderón-Romero P, Romero-Rodríguez A, Paredes-Sabja D. 2020.
608 Characterization of Exosporium Layer Variability of C*lostridioides difficile* Spores in the
609 Epidemically Relevant Strain R20291. Front Microbiol 11:1345.
610 39. Nikitas G, Deschamps C, Disson O, Niault T, Cossart P, Lecuit M. 2011. Transcytosis of
611 *Listeria monocytogenes* across the intestinal barrier upon specific targeting of goblet cell
612 accessible E-cadherin. J Exp Med 208:2263-77.
613 40. Gessain G, Tsai YH, Travier L, Bonazzi M, Grayo S, Cossart P, Charlier C, Disson O, Lecuit
614 M. 2015. PI3-kinase activation is critical for host barrier permissiveness to *Listeria*
615 *monocytogenes*. J Exp Med 212:165-83.
616 41. Pentecost M, Otto G, Theriot JA, Amieva MR. 2006. *Listeria monocytogenes* invades the
617 epithelial junctions at sites of cell extrusion. PLoS Pathog 2:e3.

618 42. Pentecost M, Kumaran J, Ghosh P, Amieva MR. 2010. *Listeria monocytogenes* internalin
619 B activates junctional endocytosis to accelerate intestinal invasion. PLoS Pathog
620 6:e1000900.
621 43. Singh B, Su YC, Riesbeck K. 2010. Vitronectin in bacterial pathogenesis: a host protein
622 used in complement escape and cellular invasion. Mol Microbiol 78:545-60.
623 44. Henderson B, Nair S, Pallas J, Williams MA. 2011. Fibronectin: a multidomain host
624 adhesin targeted by bacterial fibronectin-binding proteins. FEMS Microbiol Rev 35:147-
625 200.
626 45. Hamzaoui N, Kernéis S, Caliot E, Pringault E. 2004. Expression and distribution of beta1
627 integrins in in vitro-induced M cells: implications for *Yersinia* adhesion to Peyer's patch
628 epithelium. Cell Microbiol 6:817-28.
629 46. Clark MA, Hirst BH, Jepson MA. 1998. M-cell surface beta1 integrin expression and
630 invasin-mediated targeting of *Yersinia pseudotuberculosis* to mouse Peyer's patch M
631 cells. Infect Immun 66:1237-43.
632 47. Lecuit M, Dramsi S, Gottardi C, Fedor-Chaiken M, Gumbiner B, Cossart P. 1999. A single
633 amino acid in E-cadherin responsible for host specificity towards the human pathogen
634 *Listeria monocytogenes*. EMBO J 18:3956-63.
635 48. Mengaud J, Lecuit M, Lebrun M, Nato F, Mazie JC, Cossart P. 1996. Antibodies to the
636 leucine-rich repeat region of internalin block entry of *Listeria monocytogenes* into cells
637 expressing E-cadherin. Infect Immun 64:5430-3.
638 49. Kim M, Fevre C, Lavina M, Disson O, Lecuit M. 2020. Live Imaging Reveals Listeria
639 Hijacking of E-Cadherin Recycling as It Crosses the Intestinal Barrier. Curr Biol
640 doi:10.1016/j.cub.2020.11.041.
641 50. Diaz-Gonzalez F, Milano M, Olguin-Araneda V, Pizarro-Cerda J, Castro-Cordova P, Tzeng
642 SC, Maier CS, Sarker MR, Paredes-Sabja D. 2015. Protein composition of the outermost
643 exosporium-like layer of *Clostridium difficile* 630 spores. J Proteomics 123:1-13.
644 51. Kelly CP, Poxton IR, Shen J, Wilcox MH, Gerding DN, Zhao X, Laterza OF, Railkar R, Guris
645 D, Dorr MB. 2020. Effect of Endogenous *Clostridioides difficile* Toxin Antibodies on
646 Recurrence of *C. difficile* Infection. Clin Infect Dis 71:81-86.
647

648

649

650

Figure Legends

Figure 1. Distribution of accessible and total E-cadherin in undifferentiated and differentiated Caco-2 cells. 3D projection of a representative confocal micrograph of healthy *A*, undifferentiated, and *B*, differentiated Caco-2 cells immunostaining for accessible E-cadherin. Accessible E-cadherin (shown as acc Ecad) is in green, F-actin in red, and nuclei in blue. *C*, Repartition of positive (Ecad+) or negative (Ecad−) cells stained for accessible E-cadherin for each field. 3D projection of a representative confocal micrograph of a healthy *D*, undifferentiated and *E*, differentiated Caco-2 cells immunostaining for total E-cadherin and *F*, Repartition of cells that were positive (Ecad+) or negative (Ecad−) stained for total E-cadherin for each field. Fluorophores colors were digitally reassigned for a better representation. Micrographs are representative of 6 fields of 2 independent experiments. Scale bar, 20μm. Error bars indicate mean ± SEM. Statistical analysis was performed by two-tailed unpaired Student's *t*-test, ns, $p > 0.05$; ****, $p \leq 0.0001$.

Figure 2. The accessibility of E-cadherin increases in TcdA and TcdB intoxicated IECs. Differentiated TcdA/TcdB intoxicated Caco-2 cells for 3, 6, or 8 h in DMEM without serum. As a control, cells were incubated with DMEM without serum. Non-permeabilized cells were stained for accessible E-cadherin (shown as acc Ecad; green), permeabilized, and total E-cadherin was stained (shown as total Ecad; red) and nuclei (blue). *A*, Representative confocal microscopy images 3D (XY) projection of control cells (left) and TcdA/TcdB intoxicated cells for 8h (right); below the orthogonal view (XZ; accessible E-cadherin, total E-cadherin and merged) of the dotted line of the XY. Relative Fl.Int. measured as the sum of each z-step of *B*, accessible E-cadherin, and its abundance in the *C*, apical side, or *D* in the basal side of the cell.

Relative Fl.Int. of *E*, total E-cadherin, its abundance in the *F*, apical side, and the *G*, basal side of the cell. Controls were set 100%. Error bars indicate the mean ± SEM from at least 9 fields (n = 3). Statistical analysis was performed by two-tailed unpaired Student's *t*-test, ns, $p > 0.05$; ****, $p < 0.0001$. Bars, 5μm.

Figure 3. TcdA and TcdB increase *C. difficile* spore interaction with IECs.

Differentiated TcdA/TcdB intoxicated Caco-2 cells for 8 or incubated with DMEM without serum as control and then, were washed with PBS and infected for 3 h at an MOI 10 with *C. difficile* spores. Unbound spores were rinsed off. Non-permeabilized cells were stained for adhered spores. *A*, *B*, Representative epifluorescence microscopy images of TcdA and TcdB intoxicated cells (or DMEM as control) for 8 h then washed and infected with *C. difficile* spore. *C*, *C. difficile* spore adherence relative to the control. *D*, Internalization of *C. difficile* spores to cells. Error bars indicate the mean ± SEM from at least 9 fields (n = 3). For each bar, a total of ~4,500 - ~6,000 spores were analyzed from two different fields. Statistical analysis was performed by unpaired *t*-test, ns, $p > 0.05$. Bars, 10 μm.

Figure 4. E-cadherin of IECs interacts with *C. difficile* spores increasing in TcdA and TcdB intoxicated cells,

Differentiated Caco-2 cells were intoxicated with TcdA and TcdB for 8 h at 37 °C in DMEM without serum. As a control, cells were incubated with DMEM without serum. Then cells were infected with *C. difficile* spores for 1 h at 37 °C. Non-permeabilized cells were stained for accessible E-cadherin (shown as acc Ecad; green), spores (red), and nuclei (blue). *A*, 3D projection of a representative confocal micrograph of healthy cells infected with *C. difficile*

spores (Ctrl). On the right, magnifications of representative *C. difficile* spores associated or not with E-cadherin. *B*, *C*, Plot profile Fl.Int. of *C. difficile* spores (red line) and accessible E-cadherin (shown as Ecad, green line) performed in the white line of *A*. *D*, 3D projection of a representative confocal micrograph of TcdA and TcdB intoxicated cells infected with *C. difficile* spores. On the right magnifications of representative *C. difficile* spores associated or not with E-cadherin. *E*, *F*, Plot profile Fl.Int. of *C. difficile* spores (red) and accessible E-cadherin (shown as Ecad, in green) performed in the white line of *D*. Repartition of spores that were positive (Ecad+) or negative (Ecad−) associated with fluorescence signal for accessible E-cadherin was shown as the average associated/non-associated spores with E-cadherin for each field, a total of ~500 spores were analyzed. Fluorophores were digitally reassigned for a better representation. Micrographs are representative of 6 independent fields of 3 different experiments. Error bars indicate mean ± SEM. Statistical analysis was performed by two-tailed unpaired Student's *t*-test, ns, $p > 0.05$; **, $p \leq 0.01$; ***, $p \leq 0.001$. Bars, 10μm.

Figure 5. E-cadherin blocking antibodies decrease the spore interaction with IECs.

Undifferentiated, differentiated, and polarized Caco-2 cells were infected with *C. difficile* spores preincubated with FBS in the presence of anti-E-cadherin or non-immune IgG as control for 2 h at 37 °C. *A*, adherence, and *B*, internalization of *C. difficile* spores in undifferentiated Caco-2 cells or *C*, adherence and *D*, internalization in differentiated Caco-2. *E*, *C. difficile* spore adherence in polarized Caco-2 cells. Data shown in each panel are normalized to 0 μg mL^{-1} of antibody.

In bars, each dot represents one independent well collected from 2 independent experiments. For each bar, a total of ~1,300 spores were analyzed. Error bars indicate mean ± SEM. Statistical

analysis was performed by two-tailed unpaired Student's *t*-test, ns, $p > 0.05$; ****, $p < 0.0001$.

Figure 6. E-cadherin interacts with *C. difficile* spore.

A, Solid-phase binding test of human purified E-cadherin to 1.6×10^8 *C. difficile* spores or BSA as control, fixed on 96-well plate and incubated with increasing concentration (i.e., 0.2, 2.0, 20 and 200 nM) of human purified E-cadherin. The data represented are the mean of 9 independent wells collected in 3 independent experiments. *B*, Representative phase-contrast micrograph, immunofluorescence against E-cadherin, and immunofluorescence plot profile of 4×10^7 *C. difficile* spores that were incubated with increasing concentrations (i.e., 1, 2.5, 5, 10, 25 µg mL^{-1}) of human purified E-cadherin for 1 h at 37 °C. *C*, Quantitative analysis of Fl.Int. *D*, Distribution of E-cadherin fluorescence intensity of *C. difficile* incubated with increasing concentrations (i.e., 1, 2.5, 5, 10, 25 µg mL^{-1}) of human purified E-cadherin. A total of ~450 spores were analyzed for each condition. Error bars indicate mean ± SEM. Statistical analysis was performed by two-tailed unpaired Student's *t*-test, ns, $p > 0.05$; *, $p < 0.05$; ****, $p < 0.0001$.

Figure 7. Immunoelectron microscopy of E-cadherin-gold complex binds to *C. difficile* spores.

A - *C* TEM of *C. difficile* spores incubated with *B*, *C*, 10 µg mL^{-1} E-cadherin or *A*, without E-cadherin (negative control). Then incubated with anti-E-cadherin and anti-mouse-gold 12 nm complex. White arrows denote the mouse anti-E-cadherin and anti-mouse-gold 12 nm complex. *D*, *E* are a magnification of the black squares of *C*. *F*, Quantification of the *C. difficile* spore associated with E-cadherin ("−" and "+" denote negative or positive association, respectively). Classification of E-cadherin positively associated *C. difficile* spores according to the morphology

of the spore, thin or thick exosporium, represented as the percentage of the total E-cadherin positive spores. Figures are representative of 2 independent experiments. A total of 100 spores were quantified.

Supplementary figures

Supplementary Figure 1. Supplementary confocal micrographs of Fig. 2.

These are supplementary figures from the experiment detailed in Fig. 4. Differentiated Caco-2 cells intoxicated with 600 pM of TcdA and TcdB for 3, 6, or 8 h in DMEM without serum. As a control, cells were treated with DMEM without serum. Non-permeabilized cells were stained for accessible E-cadherin (shown as acc Ecad) in green, then permeabilized and stained total E-cadherin (total Ecad) shown in red nuclei shown in blue. Representative confocal microscopy images 3D (XY) projection of intoxicated cells for 3 h (left) or 6 h (right) with its control; below a magnified slide (XY), and the orthogonal view (XZ). Representative images from at 9 fields (*n* = 3). Bars, 5μm.

Figure 1

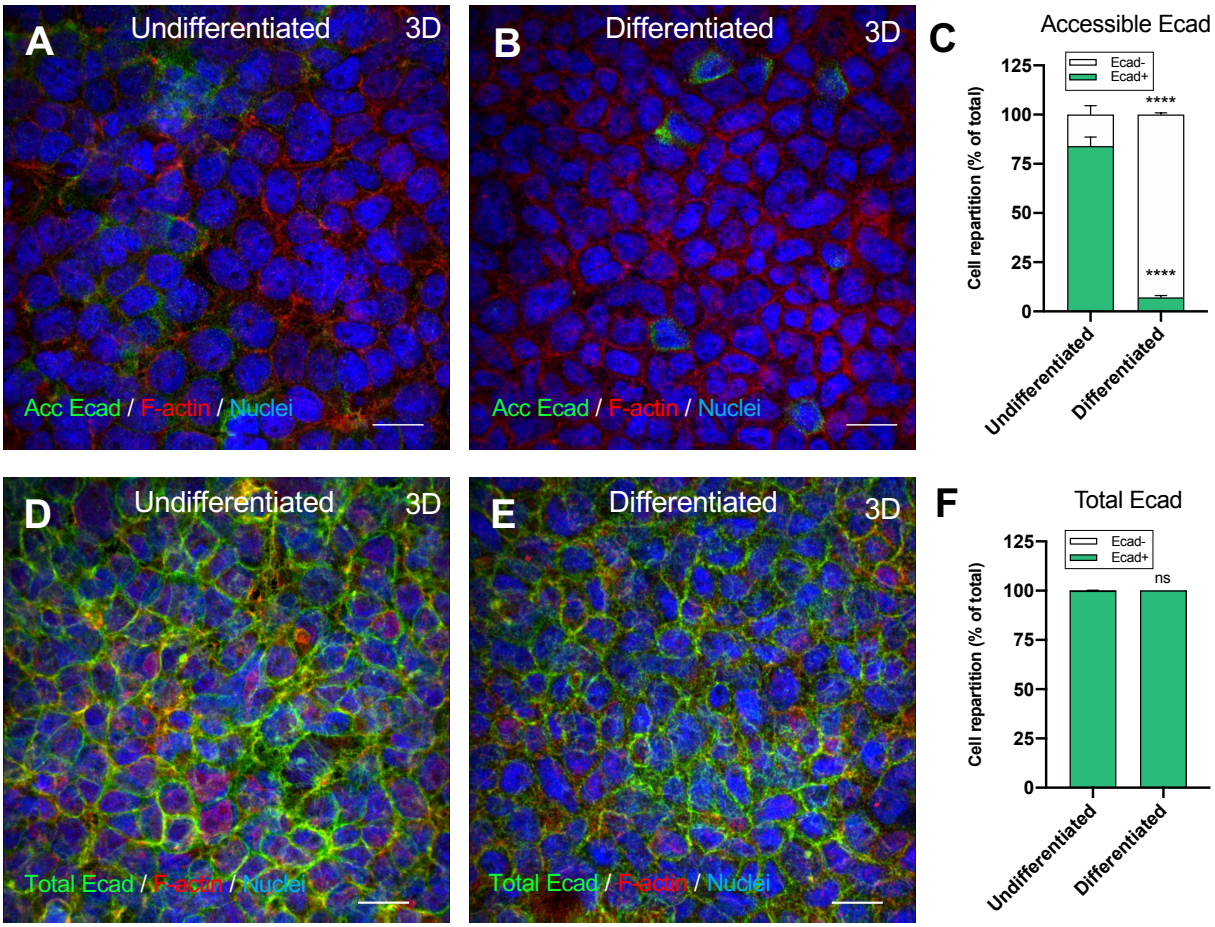
A
Undifferentiated
3D
Acc Ecad / F-actin / Nuclei
B
Differentiated
3D
Acc Ecad / F-actin / Nuclei
C
Accessible Ecad
Ecad-
Ecad+
Cell repartition (% of total)
125
100
75
50
25
0
****
****
Undifferentiated
Differentiated
D
Undifferentiated
3D
Total Ecad / F-actin / Nuclei
E
Differentiated
3D
Total Ecad / F-actin / Nuclei
F
Total Ecad
Ecad-
Ecad+
Cell repartition (% of total)
125
100
75
50
25
0
ns
Undifferentiated
Differentiated

Figure 2

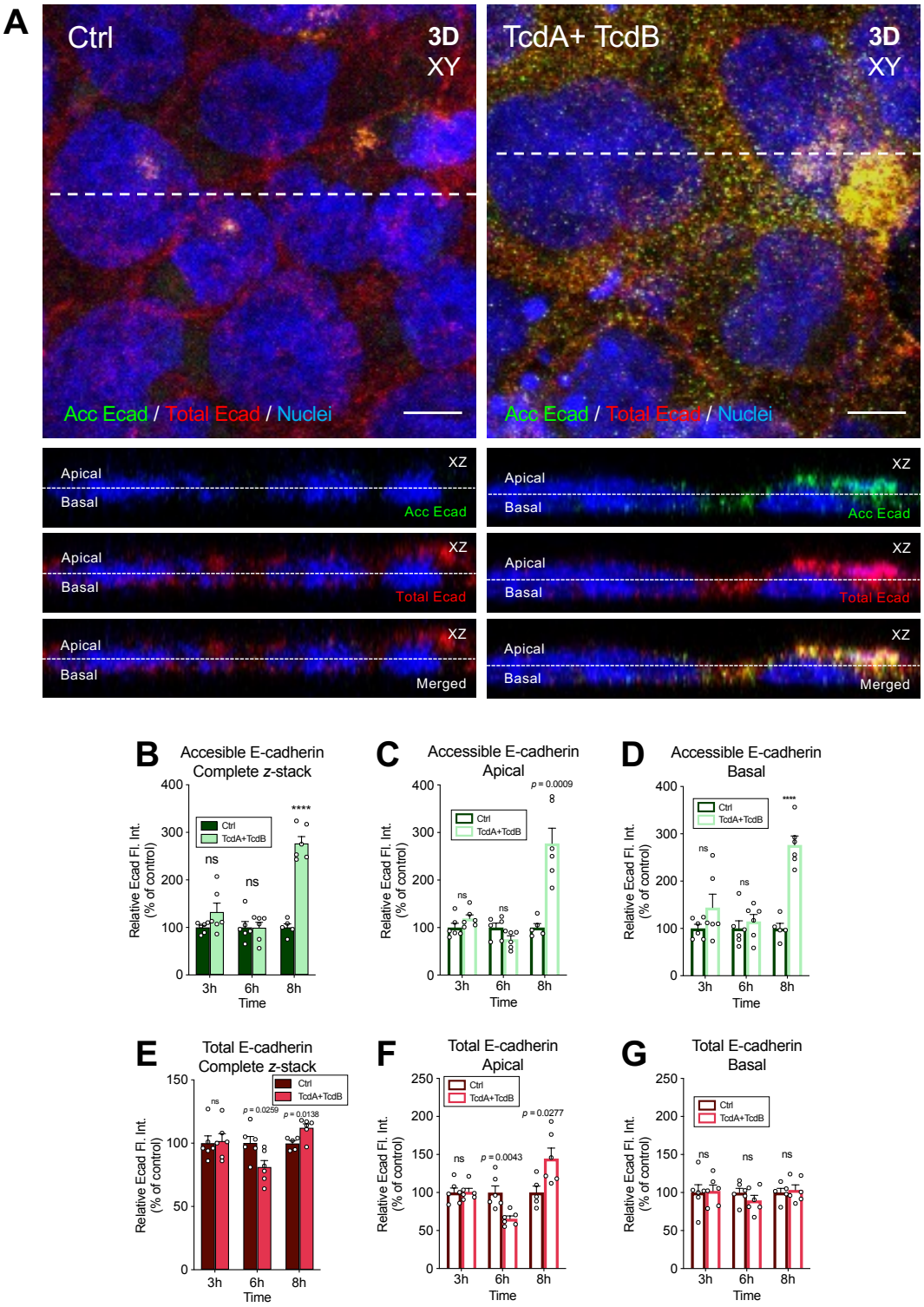
A
Ctrl
3D
XY
Acc Ecad / Total Ecad / Nuclei
TcdA+ TcdB
3D
XY
Acc Ecad / Total Ecad / Nuclei
Apical
Basal
XZ
Acc Ecad
Total Ecad
Merged
B
Accesible E-cadherin
Complete z-stack
C
Accessible E-cadherin
Apical
D
Accessible E-cadherin
Basal
E
Total E-cadherin
Complete z-stack
F
Total E-cadherin
Apical
G
Total E-cadherin
Basal
Ctrl
TcdA+TcdB
Relative Ecad Fl. Int.
(% of control)
Time
3h
6h
8h
ns
p = 0.0009
p = 0.0259
p = 0.0138
p = 0.0043
p = 0.0277
****

Figure 3

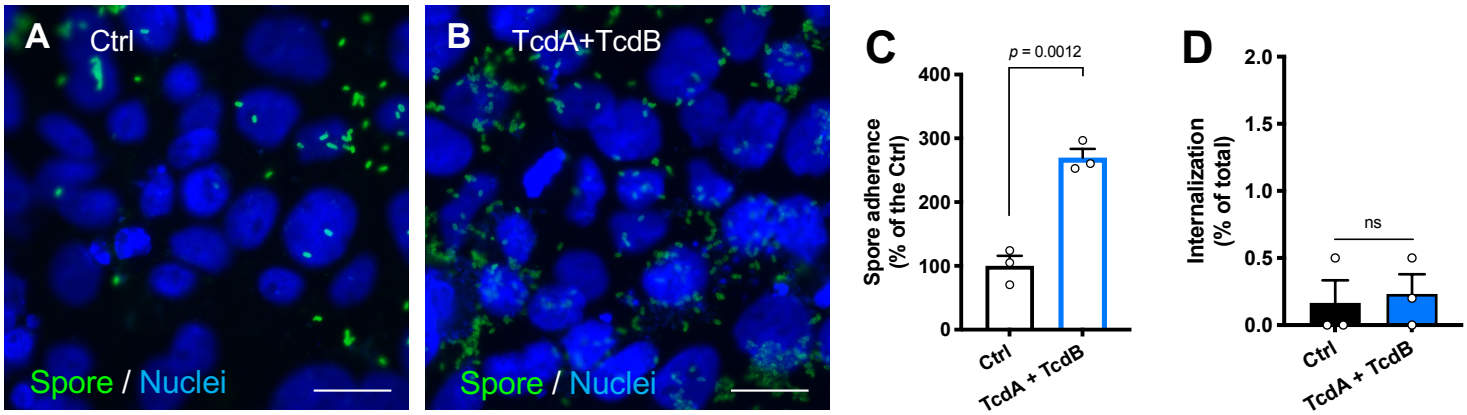
A
Ctrl
Spore / Nuclei
B
TcdA+TcdB
Spore / Nuclei
C
p = 0.0012
Spore adherence
(% of the Ctrl)
400
300
200
100
0
Ctrl
TcdA + TcdB
D
Internalization
(% of total)
2.0
1.5
1.0
0.5
0.0
ns
Ctrl
TcdA + TcdB

Figure 4

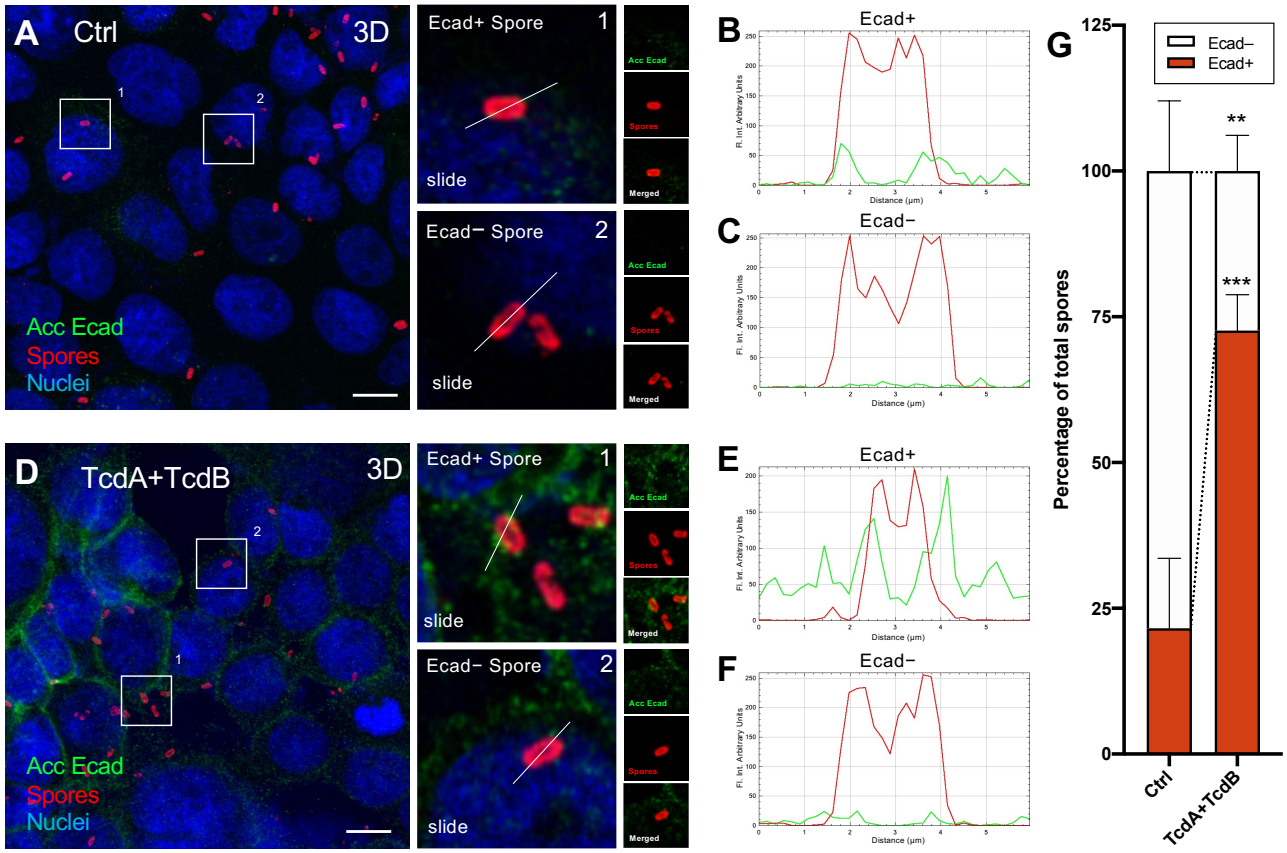
A
Ctrl
3D
Acc Ecad
Spores
Nuclei
Ecad+ Spore
1
slide
Ecad− Spore
2
slide
Acc Ecad
Spores
Merged
D
TcdA+TcdB
3D
Acc Ecad
Spores
Nuclei
Ecad+ Spore
1
slide
Ecad− Spore
2
slide
B
Ecad+
C
Ecad−
E
Ecad+
F
Ecad−
Fl. Int. Arbitrary Units
Distance (µm)
G
Ecad−
Ecad+
Percentage of total spores
125
100
75
50
25
0
**
***
Ctrl
TcdA+TcdB

Figure 5

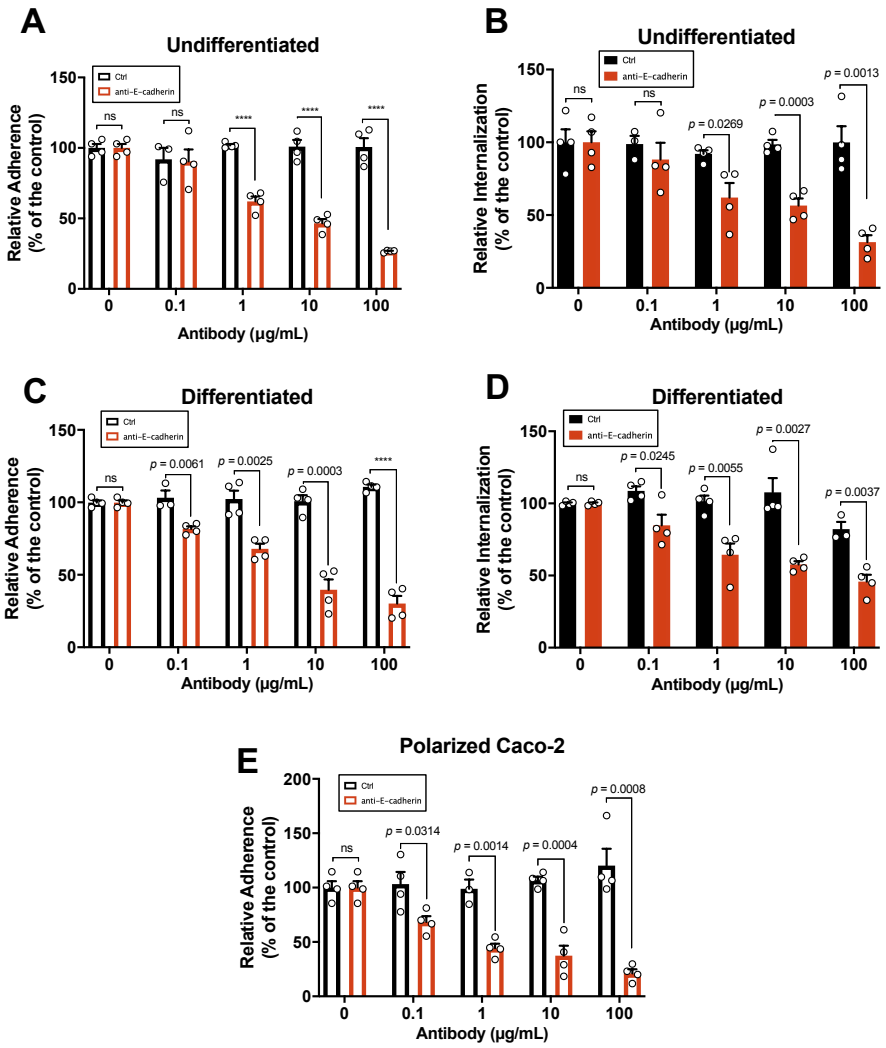
A
Undifferentiated
Ctrl
anti-E-cadherin
Relative Adherence (% of the control)
Antibody (µg/mL)
ns
ns
****
****
****
B
Undifferentiated
Relative Internalization (% of the control)
ns
ns
p = 0.0269
p = 0.0003
p = 0.0013
C
Differentiated
p = 0.0061
p = 0.0025
p = 0.0003
****
D
Differentiated
p = 0.0245
p = 0.0055
p = 0.0027
p = 0.0037
E
Polarized Caco-2
p = 0.0314
p = 0.0014
p = 0.0004
p = 0.0008

Figure 6

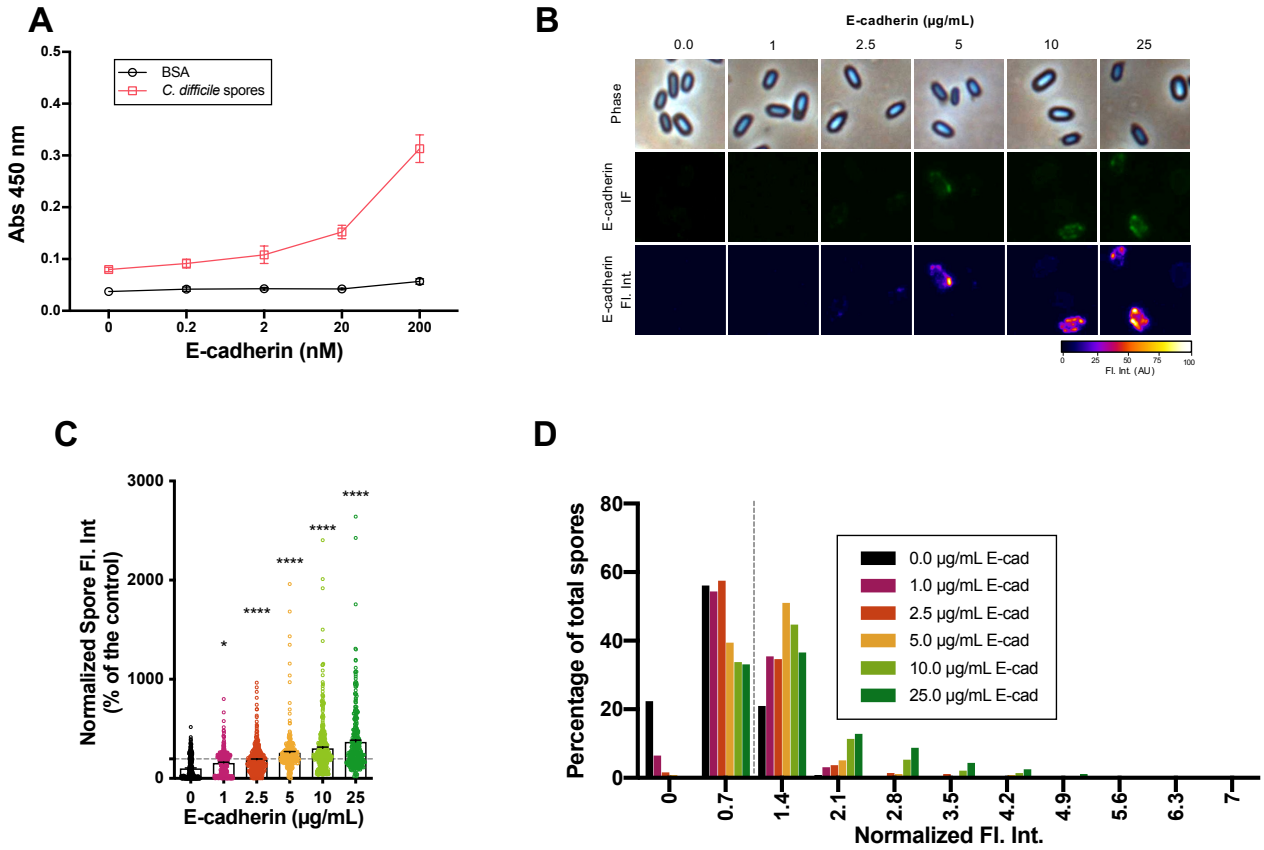
A
Abs 450 nm
0.5
0.4
0.3
0.2
0.1
0.0
BSA
C. difficile spores
0
0.2
2
20
200
E-cadherin (nM)
B
E-cadherin (µg/mL)
0.0
1
2.5
5
10
25
Phase
E-cadherin IF
E-cadherin Fl. Int.
Fl. Int. (AU)
C
Normalized Spore Fl. Int (% of the control)
3000
2000
1000
0
*
****
****
****
****
0
1
2.5
5
10
25
E-cadherin (µg/mL)
D
Percentage of total spores
80
60
40
20
0
0.0 µg/mL E-cad
1.0 µg/mL E-cad
2.5 µg/mL E-cad
5.0 µg/mL E-cad
10.0 µg/mL E-cad
25.0 µg/mL E-cad
0
0.7
1.4
2.1
2.8
3.5
4.2
4.9
5.6
6.3
7
Normalized Fl. Int.

Figure 7

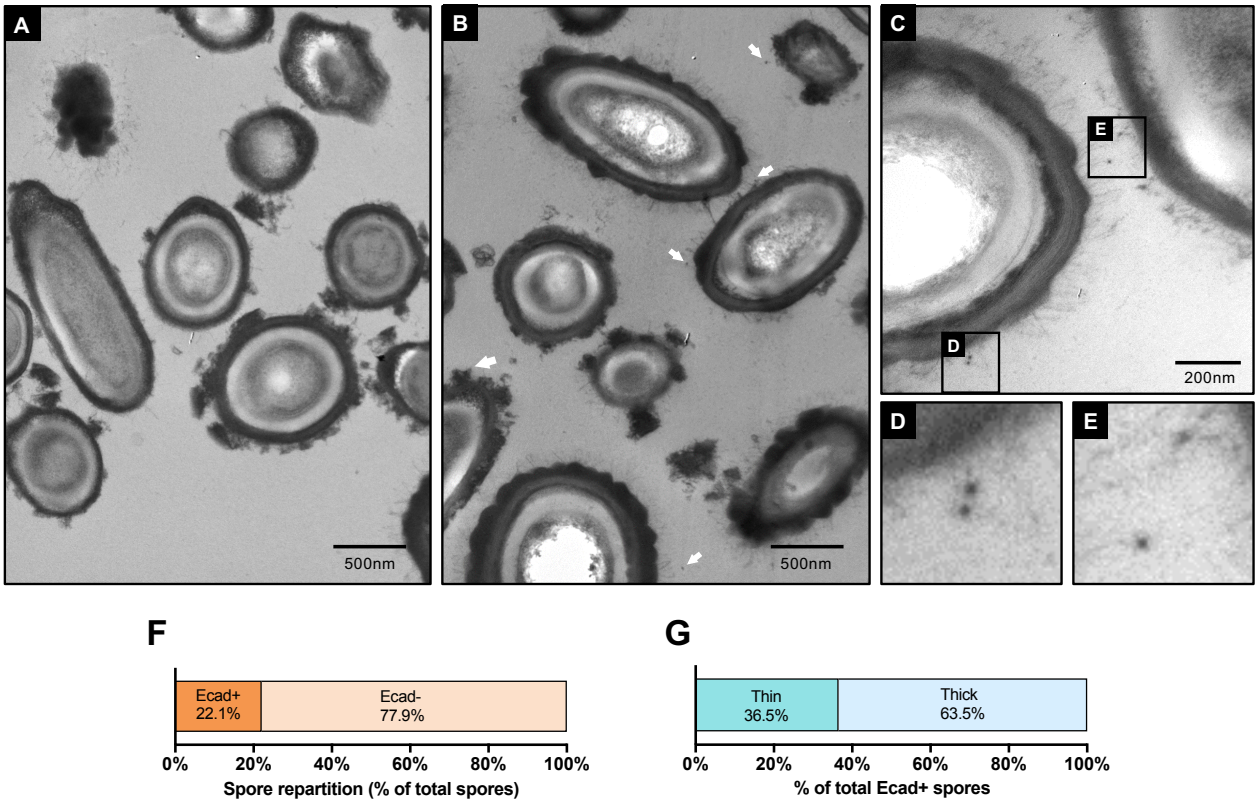
A
500nm
B
500nm
C
E
D
200nm
D
E
F
Ecad+
22.1%
Ecad-
77.9%
0%
20%
40%
60%
80%
100%
Spore repartition (% of total spores)
G
Thin
36.5%
Thick
63.5%
0%
20%
40%
60%
80%
100%
% of total Ecad+ spores
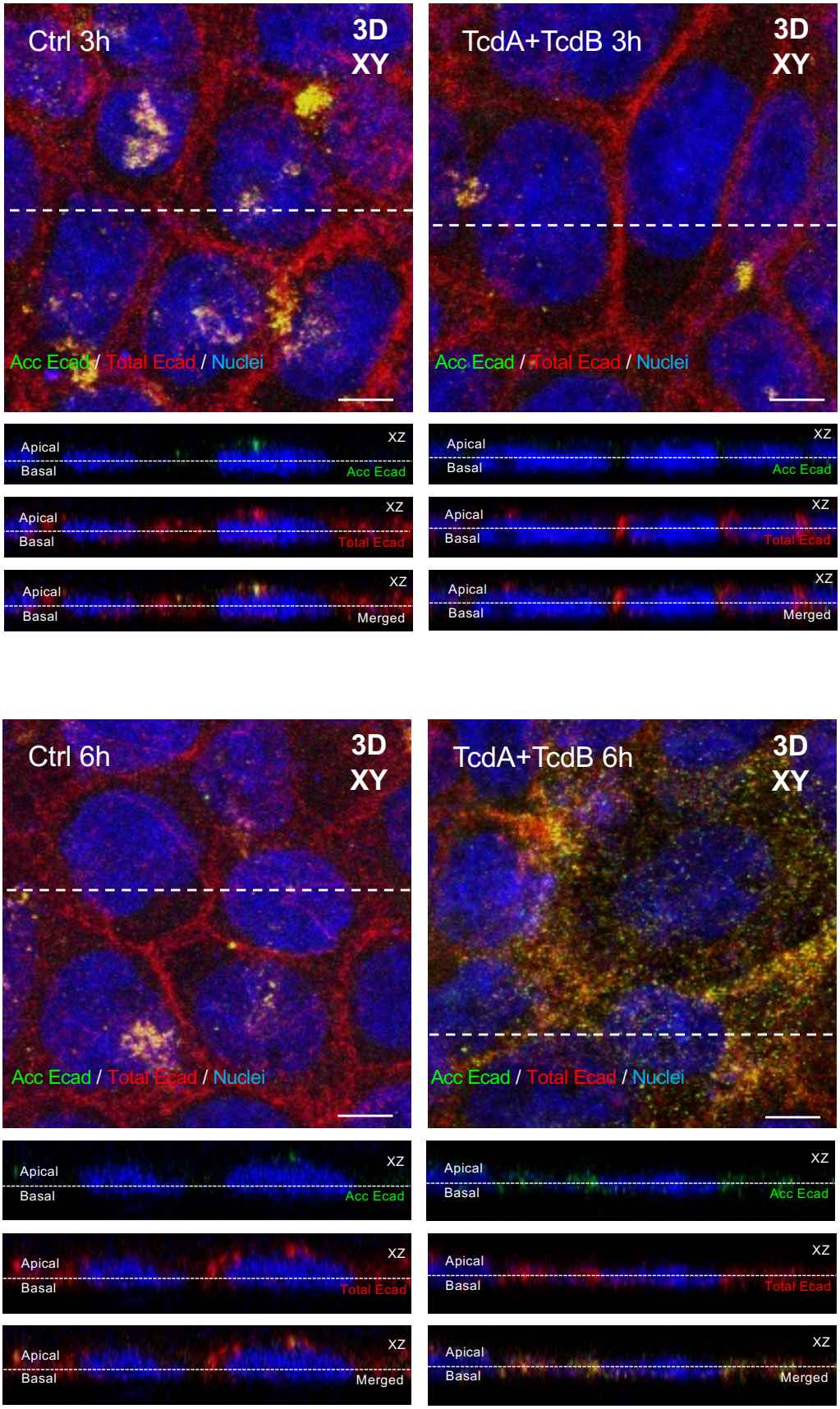
Supplementary Fig 1